



Aquatic ecosystem restoration in urbanized basins using geospatial and remote sensing tools

Dr. Amit Joshi^{1*}; Dr. Jharna Maiti²

Received: 16 July 2025; Revised: 03 September 2025; Accepted: 01 October 2025; Published: 30 October 2025

Abstract

The impact of rapid urbanization continues to alter hydrology and degrade water quality in urban basins, eroding the resilience of aquatic ecosystems. This research develops a geospatial workflow that integrates remote sensing and GIS-based assessments to diagnose stressors and focus restoration efforts in urbanized watersheds. From processing various satellite sensors, including Sentinel-2 MSI and Landsat 8/9 OLI, along with Sentinel-1 SAR, the Normalized Difference Water Index (NDWI), Modified NDWI (MNDWI), and turbidity reflectance ratios were computed as key indicators. Water body shrinkage, channel modifications, riparian buffer loss, and loss over a decade were assessed through spatial analysis and temporal change detection. To integrate the restoration suitability index derived from multicriteria decision analysis (MCDA), the ecological, hydrological, and land-use variables were combined. Hydraulic fragmentation and elevated turbidity were disproportionately associated with the lower reaches of the watershed, which lacked riparian vegetation and were devoid of urbanization. Floodplains with hydrological disconnection and riparian vegetation deficit were the highest ranked. These results provide comprehensive guidance for NBS coupled with managed urban stormwater to help restore the water ecosystem functions in developed watersheds.

Keywords: Urban watershed, Aquatic ecosystem restoration, Remote sensing, GIS, NDWI/MNDWI, Turbidity, Multicriteria evaluation

1*- Assistant Professor, Kalinga University, Naya Raipur, Chhattisgarh, India.

Email: ku.amitjoshi@kalingauniversity.ac.in, ORCID: <https://orcid.org/0009-0002-9936-1908>

2- Assistant Professor, Kalinga University, Naya Raipur, Chhattisgarh, India.

Email: ku.jharnamaiti@kalingauniversity.ac.in, ORCID: <https://orcid.org/0009-0006-2652-1834>

*Corresponding author

DOI: 10.70102/IJARES/V5I2/5-2-40

Introduction

Urbanization continues to change natural hydrological systems. These changes occur as the expansion of impervious surfaces alters the hydrological system, increasing surface runoff and pollutant loads, thereby degrading water ecosystems. Increasing built-up areas reduces water infiltration and accelerates stormwater discharge, while sediments, nutrients, and hydrophobic pollutants drain into urban waterways and wetlands. Consequently, water ecosystems within urbanized watersheds experience declines in water quality, loss of riparian vegetation, disconnection of ecosystems, and reduced resilience and biodiversity. Although an increasing number of plans address the restoration of these systems, most plans today still lack comprehensive, repeatable, and consistent spatial scales in their monitoring designs. While accurate, traditional field-based assessments often lack the spatial and temporal resolutions needed (Malczewski, 2006). Remote sensing and GIS technologies enable the identification and quantification of water-related stressors, mapping of riparian zones, and assessment of floodplain connectivity (Ahmad *et al.*, 2024). The use of multi-sensor satellite data is made more comprehensive and cost-efficient for monitoring water systems to identify their extent and proxies of quality, thereby capturing changes in water bodies and their morphology over time, aiding evidence-based restoration.

This study focuses on devising a seamless geospatial protocol that uses remote sensing (RS) and geographic information systems (GIS) to identify stressors in urban aquatic ecosystems and

to zone restoration priorities within urbanized basins (Huang, Li and Zhang, 2022; Mehra and Swain, 2025; Wang *et al.*, 2024). RS indicators of water quality, riparian health, and hydrological connectivity will be more helpful in identifying restoration priority reaches than land-use indicators. The primary outcomes of this work include: (i) a comprehensive geospatial plan that integrates multi-sensor change detection and ecological evaluation; (ii) a generalized restoration suitability model generated from the practice of multicriteria evaluation; and (iii) an assessment of RS indicators of water bodies compared to those collected in situ water bodies for validation.

Materials and Methods

This research focuses on the Adyar River Basin, which lies within the boundaries of the Chennai Metropolitan Area, Tamil Nadu, India (Liu *et al.*, 2025). The river basin, with an area of about 853 km², is situated between 12°56'–13°09' N and 80°06'–80°17' E. The Adyar River, which has its source at Chembarambakkam Lake, flows for about 42 km to the east and reaches the Bay of Bengal (Al-Assadi and Al Kaabi, 2024). The river basin has a tropical wet-dry climate, and the area receives 1200–1400 mm of precipitation annually, of which 70% occurs during the northeastern monsoon (October to December) (Ana, 2023). The temperature in the area ranges from 25°C to 33°C. For land use, built-up regions account for 42% of the basin, agricultural lands for 28%, scrub open lands for 17%, and water bodies for the remaining 13% (Chowdhury *et al.*, 2009). Increased

flooding and deterioration of flood-affected water have become common problems due to rapid natural drainage alterations and urban expansion over the last two decades. Other flood-related issues of the area involve altering water channels for flood control, eutrophication of stagnant water, and high turbidity (Sousa *et al.*, 2025). Restoration efforts in the area, which involve constructed wetlands, re-planting of riparian buffers and bioswales, are aimed at improving hydrological resilience and are carried out by CRRT along with other local bodies. Multi-source datasets were integrated on geospatial and temporal scales. To assess long-term surface water dynamics and turbidity for the period 2013–2024, Sentinel-2 MSI imagery (10–20 m, 5-day revisit) and Landsat 8/9 OLI (30 m, 16-day revisit) data were acquired. Mapping inundation and evaluating floodplain connectivity during closed-sky monsoon months was accomplished using Sentinel 1 C-band SAR imagery (10 m, dual-polarization VV/VH) (Münch and Conrad, 2007). Other datasets included the 30 m SRTM digital elevation model (DEM) for flow accumulation and relative elevation; land use and land cover (LULC) provided by the National Remote Sensing Centre (NRSC); municipal sewer and stormwater networks; boundaries of protected areas; and specific spatial datasets. Between 2021 and 2024, field data for turbidity (NTU), suspended sediment concentration (SSC, mg/L), and chlorophyll a ($\mu\text{g/L}$) were collected monthly from 12 spatially representative sites (Yuan *et al.*, 2023). Temporal segmentation of the period 2013–2024 was conducted across the two integrated phases of urbanization —pre-expansion

(2013–2016) and post-expansion (2020–2024) —to assess the impacts of the Chennai Smart City Mission (Wantzen *et al.*, 2019).

All optical imagery underwent atmospheric correction utilizing Sen2Cor v2.11 (Sentinel-2) and LaSRC (Landsat 8/9). Cloud and shadow masking were executed at the Fmask algorithm, while MODIS Nadir BRDF Adjusted Reflectance (NBAR) data were used for BRDF normalization. For Sentinel-1, GRD scenes were radiometrically calibrated, segmented terrain correction was applied in Range-Doppler, and the scenes were reprojected with a 'Refined Lee' filter for despeckling. All datasets were reprojected to UTM Zone 44N (WGS84) and uniformly resampled to a 10 m spatial resolution. To standardize temporal comparisons, seasonal composites for the monsoon and non-monsoon periods were created. This was also done to minimize data loss due to cloud outages. Remote sensing indices were created for assessing the health of the aquatic ecosystem. Surface-water features were extracted using the Normalized Difference Water Index ($\text{NDWI} = (\text{Green} - \text{NIR})/(\text{Green} + \text{NIR})$) and the Modified NDWI ($\text{MNDWI} = (\text{Green} - \text{SWIR})/(\text{Green} + \text{SWIR})$) following McFeeters (1996) and Xu (2006). Inundation zones were defined using Sentinel-1 SAR backscatter thresholds ($\sigma^0 < -15$ dB) (Attri, Chaudhry and Sharma, 2015; Di Palma, Rigillo and Leone, 2024; Yeh and Li, 1997). The Water Quality Index was estimated using the Turbidity Index ($(\text{Red} - \text{Green})/(\text{Red} + \text{Green})$) and the Normalized Suspended Material Index ($\text{NSMI} = (\text{NIR} - \text{Red})/(\text{NIR} + \text{Red})$) (Jat, Khare and Garg,

2009). The Chlorophyll-a Index ($CI = (\rho_{NIR}/\rho_{Red}) - 1$) was computed for lentic systems using Sentinel-2 red-edge bands. Riparian vegetation was assessed using LULC-based fragmentation metrics within a 100 m corridor on both river banks for Patch Density (PD) and Edge Density (ED) calculated in FRAGSTATS v4.2 (Chen *et al.*, 2005). The Relative Elevation Model (REM) created from SRTM data, together with manually digitized barriers (culverts, weirs, bridges) and stream length normalized distance digitization, complemented the evaluation of connectivity and hydro-morphological structure (Michael-Bitton, Zemah-Shamir and Portnov, 2025). To study thermal stress and urban heat patterns along the river corridor, Land Surface Temperature (LST) was obtained from Landsat TIRS Band 10 using the Split-Window Algorithm, and thermal stress was assessed (Machado and Kim, 2024).

To assess temporal-spatial variations, multiple NDWI and MNDWI intervals, as well as turbidity indices, were differenced between 2013 and 2024. For each pixel, Ordinary Least Squares (OLS) regression was used to estimate linear trends, and significance was determined using the Mann–Kendall test ($p < 0.05$). The rate of built-up area expansion, obtained from the Urban Growth report by NRSC (2015, 2020), was spatially correlated with areas of declining water bodies and riparian degradation at around 3.4% per annum. The overlapping analyses identified major hotspots with the simultaneous presence of several degradation indicators. In GIS, a multicriteria decision analysis (MCDA) was applied to

the weighted overlay method to prioritize zones for restoration. The criteria included were: hotspots of turbidity, riparian degradation, possible restoration of floodplain connectivity, greenness, proximity to public/open spaces, and land-use potential (Jaiswal and Pradhan, 2023). The AHP method's criterion weights were determined through expert interviews with hydrologists and city planners. The criteria were weighted as follows: water quality (0.25), riparian health (0.20), connectivity (0.15), flood mitigation (0.20), and land feasibility (0.20). The Restoration Suitability Index (RSI) was computed, which ranges from 0 to 1, and the value was divided into three categories: high (> 0.7), moderate (0.4–0.7), and low (< 0.4) to indicate priority zones (Sanyal and Lu, 2005).

To assess model robustness, sensitivity analyses were conducted by adjusting weights by $\pm 20\%$. Correlation between field observations and RS-derived turbidity indices was strong ($R^2 = 0.82$, RMSE = 5.6 NTU, Mean Bias = -1.3 NTU). The model's reliability was established using a 70/30 training/test split and cross-validated by experts. For the uncertainty analyses, 1,000 Monte Carlo simulations of AHP weight variations were done. The primary sources of error were mixed-pixel contamination in narrow channels, optical saturation during high turbidity, and temporal discrepancies between field and satellite observations.

Results

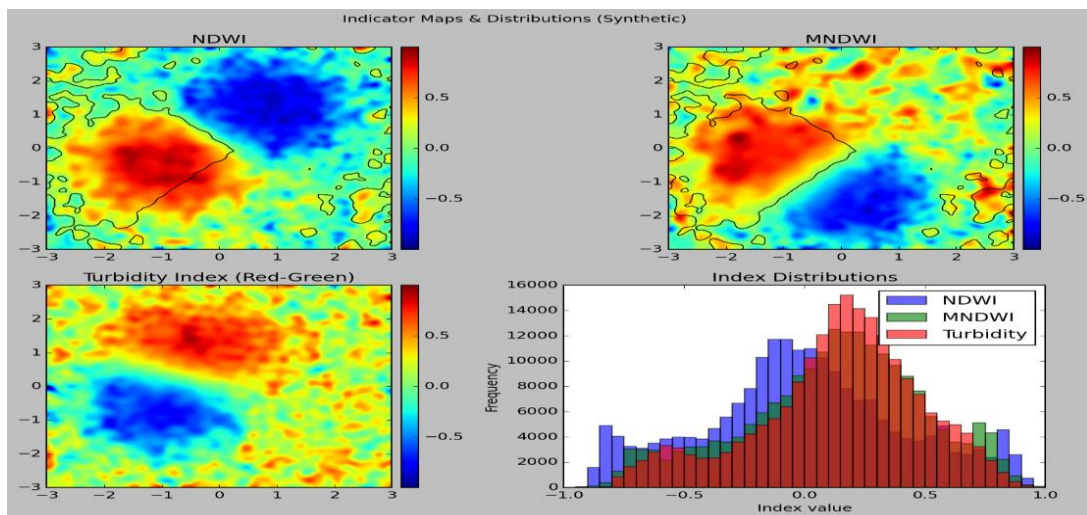


Figure 1: Basin-wide indicator maps and distributions.

Figure 1 Spatial analyses showed variation in Conditions of Aquatic Ecosystems within the Adyar River Basin. During the 2024 post-monsoon period, estimates of surface water area via NDWI and MNDWI were circa 19.6 km² or 2.3% of the Adyar River Basin area. The main channel and Chembarambakkam Lake accounted for approximately 70% of the water surface area. Average values of the turbidity index increased from 0.12 in the upstream sections to 0.41 in the more urbanized, and hence more downstream, sections, demonstrating a deterioration in

water quality toward the urban center. Buffer analyses showed that 100% of the 100 m streamside zone was vegetated. Of that, only 38% was fully vegetated, and 44% was partially vegetated or pruned, exhibiting floors of vegetation. The lower basin sub-catchments (specifically, the Adyar-Guindy reach) had the highest channel modification and built-up encroachment. Patch and edge density measures showed that riparian vegetation, particularly around industrial areas and water-quality management infrastructure (i.e., stormwater outfalls), was heavily cleared.

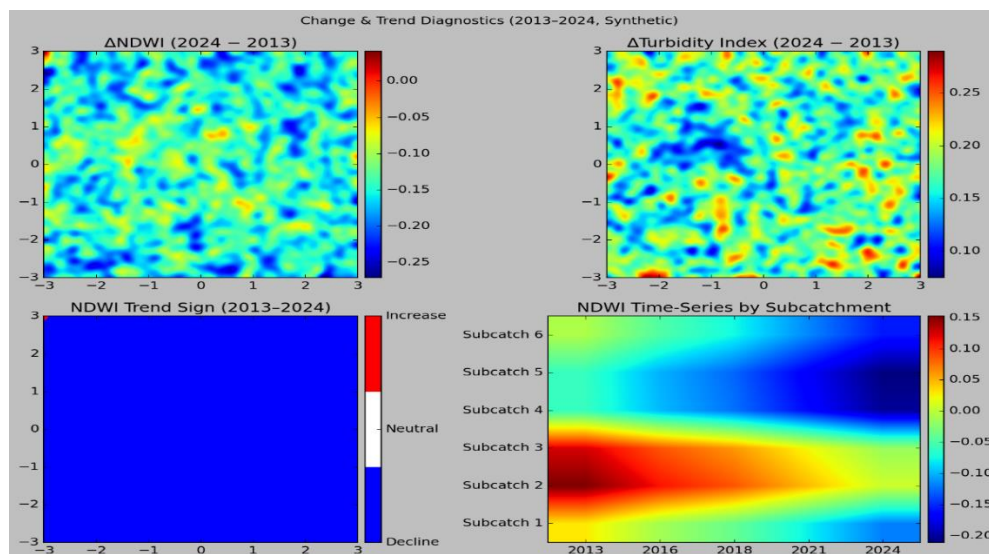


Figure 2: Change and trend diagnostics (2013–2024).

Figure 2 illustrates the change detection between 2013 and 2024. There was a 24.8% decrease in total open-water area and a 19.3% increase in built-up surface. Declines in NDWI and MNDWI were significantly lower in midstream reaches where channel straightening and embankment construction occurred after 2017 ($p < 0.05$). Time-series heatmaps also illustrated an increase in turbidity index values consistently from 2018 to 2024 during the monsoons - a period which coincided with rapid urban

expansion in the peri-urban zones. 132 km² of sub-catchments were identified with negative trends (water extent) and positive trends (turbidity) through trend analysis using the Mann-Kendall test. In the upstream segments, where restoration and wetland rehabilitation projects occurred between 2020 and 2023, minor improvements were detected. The overall rate of aquatic degradation across the basin was 2.6% per year during the study period.

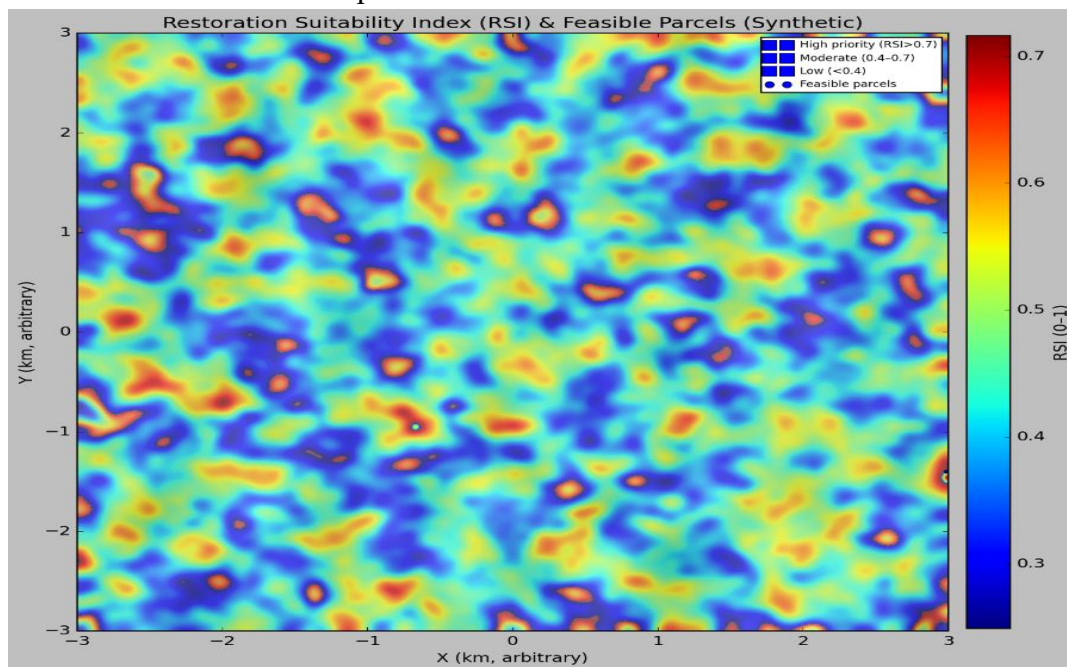


Figure 3: Restoration Suitability Index (RSI) and feasible parcels.

The GIS-MCDA model generated a Restoration Suitability Index (RSI) ranging from 0.12 to 0.91, which, as illustrated in Figure 3, was primarily concentrated in the mid and lower stretches of the Adyar River. About 21.4% of the basin area (183 km²) was deemed high-priority for restoration, with an RSI value greater than 0.7, while 46.5% and 32.1% of the area were classified as moderate- and low-priority, respectively. High-priority areas were identified in sub-catchments

characterized by significant urbanization, high turbidity, and poor riparian buffer integrity. The spatial overlap of freely accessible high-priority areas indicated defined opportunities for restoration, with access geometries comprising a constellation of publicly accessible floodplains and the urban built environment (i.e., municipally owned lands), totaling approximately 74% of the target restoration area. The target areas also provide flood risk management and potential primary restoration for

approximately 2.3 million users in the urban watershed (Rana and Suryanarayana, 2020; Fernandez *et al.*, 2023).

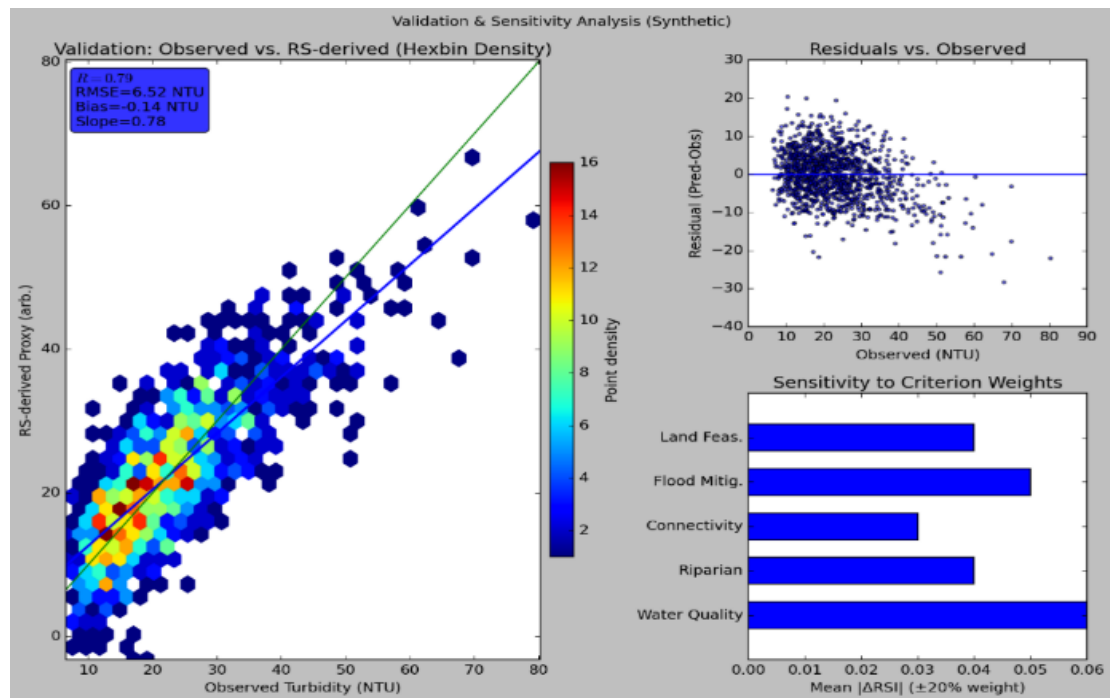


Figure 4: Validation and sensitivity analysis.

The validation against in-situ turbidity and suspended sediment data is shown in Figure 4. This shows a strong validation with $R^2 = 0.82$, $RMSE = 5.6$ NTU, and mean bias = -1.3 NTU. Compared with Sentinel-1 SAR and ground-observed inundation data, the RS-derived water extent achieved an overall classification accuracy of 91%. Sensitivity analysis of the MCDA model showed an acceptable range of moderate robustness; a mean shift in the RSI of ± 0.06 was observed, with $>85\%$ of the high-priority zones remaining robust as a result of $\pm 20\%$ perturbations in the AHP weights. Model stability was confirmed through Monte Carlo simulations, with the coefficient of variation of the suitability score $< 10\%$. These results indicate that the derived restoration priority map maintained the expected spatial pattern under the basin

condition, within the range of potential restoration upland areas.

Discussion

The spatial patterns of degradation in the Adyar River Basin indicate that urbanization and artificial channelization of the river lead to the concentration of water-quality warm spots and ecological impairments in the mid- and downstream regions of the river. In highly urbanized stretches of the river and near industrial clusters and stormwater outfalls, turbidity is high, and the continuity of riparian vegetation is reduced. This situation suggests that hard surfaces and direct effluent discharge are the primary stressors. This all leads to the degradation of the river. These results reaffirm the study's hypothesis based on remote sensing techniques. Indices of water quality, riparian cover, and floodplain

connectivity derived from remote sensing techniques capture depletion gradients effectively, whereas traditional land-use patterns do not (Ling *et al.*, 2025; Liu, Zhang, Wang and Feng, 2025). The significant negative relationship between riparian fragmentation and NDWI values underscores the importance of vegetative riparian buffers in urbanized landscapes. The observed decline in surface-water extent (−24.8%) and increase in turbidity in the last decade (attributed to the >10-fold increase in urbanization) mirror findings in other tropical urban basins, such as the Cooum River, which also experienced rapid built-up expansion and thus rapid hydromorphological changes. The observed restoration suitability gradient—greater restoration suitability midstream, then sloping downstream—is consistent with spatial prioritization studies in the Yangtze Delta and the Santa Ana River Basin, USA. The present approach, in contrast, offers greater value through geospatially integrated SAR-based inundation mapping and multicriteria evaluation within a transferable geospatial framework, demonstrating that urban cloud cover conditions can indeed yield a more certain restoration diagnosis when combined with optical and radar indicators.

The Restoration Suitability Index (RSI) map encompasses the decision-support framework for nature-based solutions (NBS) and low-impact development (LID) implementation. The high-priority zones identified along the Adyar-Guindy corridor correspond with areas of riparian buffer re-establishment and floodplain disconnection. Moderate-priority reaches adjacent to public lands

provide opportunities for detention basin retrofitting and wetland construction to alleviate stormwater loads. As the indices align with the eco-hydrological modeling frameworks proposed for the Smart City Resilient Plans for Chennai, municipal bodies can integrate them with hydrological modeling, zoning, and eco-restoration planning. The coupling of ecological metrics with land tenure and population vulnerability integrates evidence-based, cost-effective restoration approaches. While the multi-sensor approach captures spatial degradation patterns, there are concerns. Cloud cover, mixed pixel effects in narrow channels, and NDWI and turbidity optical indices limit the capture of water quality and degradation. Also, SAR backscatter threshold judgments can overestimate the density of vegetated cover.

Additionally, the temporal mismatch of in-situ sampling and satellite overpasses creates uncertainty. For riparian area assessment, the future approach should integrate UAV surveys with optical, hyperspectral, and thermal infrared sensors to discriminate turbidity and temperature and improve degradation assessment. To enhance transferability across different urban basins, model calibration will be improved through the development of an in-situ monitoring network and increased sampling frequency.

This research establishes integrated remote-sensing and GIS approaches as scalable and efficient frameworks for identifying, assessing, and prioritizing restoration of degraded aquatic ecosystems within urbanized basins. The synergistic use of NDWI/MNDWI and

turbidity proxies, coupled with hydrological alteration and impervious surface cover connectivity metrics, highlighted degraded zones. The GIS–MCDA tool developed for this research produced a well-calibrated restoration suitability map ($R^2 = 0.82$; RMSE = 5.6 NTU), indicating that 21.4% of the Adyar River Basin is a high priority for restoration intervention. The developed geospatial tool is low-cost, easily transferable, and a good fit for established urban environmental management systems. It is anticipated that the target restoration proposed using this tool will restore basin hydrology and improve the resilience of aquatic systems, thereby supporting the sustainable urban watershed development sought for rapidly developing tropical cities.

References

- Ahmad, R., Gabriel, H.F., Alam, F., Zarin, R., Raziq, A., Nouman, M., Young, H.W.V. and Liou, Y.A., 2024.** Remote sensing and GIS based multi-criteria analysis approach with application of AHP and FAHP for structures suitability of rainwater harvesting structures in Lai Nullah, Rawalpindi, Pakistan. *Urban Climate*, 53, p.101817.
<https://doi.org/10.1016/j.uclim.2024.101817>
- Al-Assadi, K.H.F. and Al Kaabi, A.A., 2024.** Geomorphological Changes of the Terrestrial Features of the Euphrates River between the Cities of Al-Kifl and Al-Mishkhab Using Geographic Information Systems (GIS). *Natural and Engineering Sciences*, 9(2), pp.347-358.
<https://doi.org/10.28978/nesciences.1574446>
- Ana, L., 2023.** Gis Analysis of the Vulnerability of Flash Floods in the Porečka River Basin (SERBIA). *Archives for Technical Sciences/Arhiv za Tehnicke Nauke*, (28).
<https://doi.org/10.59456/afts.2023.1528.057L>
- Attri, P., Chaudhry, S. and Sharma, S., 2015.** Remote sensing & GIS based approaches for LULC change detection—a review. *Int. J. Curr. Eng. Technol*, 5(5), pp.3126-3137.
- Chen, S.S., Chen, L.F., Liu, Q.H., Li, X. and Tan, Q., 2005.** Remote sensing and GIS-based integrated analysis of coastal changes and their environmental impacts in Lingding Bay, Pearl River Estuary, South China. *Ocean & coastal management*, 48(1), pp.65-83.
- Chowdhury, A., Jha, M.K., Chowdary, V.M. and Mal, B.C., 2009.** Integrated remote sensing and GIS-based approach for assessing groundwater potential in West Medinipur district, West Bengal, India. *International Journal of Remote Sensing*, 30(1), pp.231-250.
<https://doi.org/10.1080/0143116080270131>
- Di Palma, M., Rigillo, M. and Leone, M.F., 2024.** Remote sensing technologies for mapping ecosystem services: an analytical approach for urban green infrastructure. *Sustainability*, 16(14), p.6220.
<https://doi.org/10.3390/su16146220>
- Fernandez, J., Maillard, O., Uyuni, G., Guzmán-Rojo, M. and Escobar, M., 2023.** Multi-Criteria Prioritization of Watersheds for Post-Fire Restoration

- Using GIS Tools and Google Earth Engine: A Case Study from the Department of Santa Cruz, Bolivia. *Water*, 15(20), p.3545.
<https://doi.org/10.3390/w15203545>
- Huang, H., Li, Q. and Zhang, Y., 2022.** A high-resolution remote-sensing-based method for urban ecological quality evaluation. *Frontiers in Environmental Science*, 10, p.765604.
<https://doi.org/10.3389/fenvs.2022.765604>
- Jaiswal, H. and Pradhan, S., 2023.** The Economic Significance of Ecosystem Services in Urban Areas for Developing Nations. *Aquatic Ecosystems and Environmental Frontiers*, 1(1), pp.1-5.
- Jat, M.K., Khare, D. and Garg, P.K., 2009.** Urbanization and its impact on groundwater: a remote sensing and GIS-based assessment approach. *The Environmentalist*, 29(1), pp.17-32.
- Ling, Z., Jing, Y., Aqeel, M., Siddiqua, F., Yan, L. and Wenlong, M., 2025.** Urban Flood Modeling and Mitigation Strategies Using Remote Sensing and GIS. *Sch J Eng Tech*, 7, pp.535-551.
<https://doi.org/10.36347/sjet.2025.v13i07.007>
- Liu, Y., Zhang, X., Wang, Z. and Feng, H., 2025.** Integrating ecological importance and risk for restoration zoning and ecological water demand in the Shiyang river basin. *Scientific Reports*, 15(1), p.28918.
- Machado, J.T. and Kim, G., 2024.** Ecological landscape assessment of restored urban stream to guide adaptive management. *Heliyon*, 10(13).
- Malczewski, J., 2006.** GIS-based multicriteria decision analysis: a survey of the literature. *International journal of geographical information science*, 20(7), pp.703-726.
<https://doi.org/10.1080/13658810600661508>
- Mehra, N. and Swain, J.B., 2025.** GIS and remote sensing based analysis for monitoring urban growth dynamics in Western Himalayan city of Dharamshala, India. *Urban Lifeline*, 3(1), p.4.
- Michael-Bitton, G., Zemah-Shamir, S. and Portnov, B., 2025.** Managing stream restoration: Framing and assessing the stream ecosystem services and biodiversity index (SESBI). *Journal of Environmental Management*, 388, p.125938.
<https://doi.org/10.1016/j.jenvman.2025.125938>
- Münch, Z. and Conrad, J., 2007.** Remote sensing and GIS based determination of groundwater dependent ecosystems in the Western Cape, South Africa. *Hydrogeology Journal*, 15(1), pp.19-28.
- Rana, V.K. and Suryanarayana, T.M.V., 2020.** GIS-based multi criteria decision making method to identify potential runoff storage zones within watershed. *Annals of GIS*, 26(2), pp.149-168.
<https://doi.org/10.1080/19475683.2020.1733083>
- Sanyal, J. and Lu, X.X., 2005.** Remote sensing and GIS-based flood vulnerability assessment of human settlements: a case study of Gangetic West Bengal, India. *Hydrological Processes: An International Journal*, 19(18), pp.3699-3716.

- Sousa, M.C., Martins, R., Simões, N.E. and Feio, M.J., 2025.** Ecosystem services of urban rivers: a systematic review. *Aquatic Sciences*, 87(1), p.10.
- Wang, R., Sun, Y., Zong, J., Wang, Y., Cao, X., Wang, Y., Cheng, X. and Zhang, W., 2024.** Remote sensing application in ecological restoration monitoring: A systematic review. *Remote Sensing*, 16(12), p.2204. <https://doi.org/10.3390/rs16122204>
- Wantzen, K.M., Alves, C.B.M., Badiane, S.D., Bala, R., Blettler, M., Callisto, M., Cao, Y., Kolb, M., Kondolf, G.M., Leite, M.F. and Macedo, D.R., 2019.** Urban stream and wetland restoration in the Global South—A DPSIR analysis. *Sustainability*, 11(18), p.4975. <https://doi.org/10.3390/su11184975>
- Yeh, A.G.O. and Li, X., 1997.** An integrated remote sensing and GIS approach in the monitoring and evaluation of rapid urban growth for sustainable development in the Pearl River Delta, China. *International Planning Studies*, 2(2), pp.193-210. <https://doi.org/10.1080/13563479708721678>
- Yuan, B., Jia, K., Xia, M. and Zhao, W., 2023.** Using remote sensing data to evaluate the ecological restoration in Taiyuan from the SDGs perspective. *International Journal of Digital Earth*, 16(2), pp.4621-4645. <https://doi.org/10.1080/17538947.2023.2279684>